Multi-Factor Coupled Energy-Saving Optimization Strategies for Prefabricated Concrete Substation Buildings

Bin Tan[1,*], Kun Zhou[2] , Zhenhua Li[1] , Chang He[3], Yuhuan Yan[4]

[1]Economic and Technical Research Institute of State Grid Hunan Electric Power Co., Ltd, Changsha China
[2]Hunan Economic Research Electric Power Design Co., Ltd, Changsha China
[3]School of Civil Engineering, Central South University, Changsha China
[4]China Construction Fifth Engineering Bureau Co., Ltd, Changsha China

*Bin Tan: 1282554608@qq.com; Tel.:+8613975802705

Abstract. Substations play a vital role in the control and transmission of electric power; however, research on optimizing the energy efficiency of such buildings remains limited. To better understand the mechanisms of heating and cooling loads in substations, and to compare the differences in heat transfer performance between concrete and steel structures, this study seeks to propose reasonable design strategies to reduce the heating and cooling energy consumption of substations. A standardized prefabricated substation energy model was established using the Grasshopper parametric design platform in Rhino7. With the aid of the Ladybug Tools suite, and based on both the Hype and NSGA-II algorithms, single-factor energy-saving studies were conducted on different design variable combinations of this standardized substation across four representative climate zones in China, from north to south. Additionally, a multi-factor coupled optimization case study was carried out in one of these cities. The results not only reveal the energy-saving patterns of substation buildings across various climate zones but also provide reference strategies for the energy-efficient design optimization of prefabricated concrete substations under multi-factor coupling.

Keywords: Concrete substation buildings; Building energy efficiency; Multi-factor coupled optimization; Hype algorithm; NSGA-II algorithm

1 Introduction

Substations are buildings designed to transform voltage. For example, electric power transmitted via high-voltage lines to residential areas must pass through substations to be stepped down before being supplied for public use. According to the State Grid Corporation of China Development Strategy Outline [1], in order to improve overall operational efficiency, more than 7,000 new and expanded substations are planned for construction in China. At present, substations worldwide are predominantly steel structures, which offer advantages such as lighter self-weight, ease of construction, and good

S. Sing et al. (eds.), *Proceedings of the 2025 7th International Conference on Civil Architecture and Urban Engineering (ICCAUE 2025)*, Atlantis Highlights in Engineering 43,
https://doi.org/10.2991/978-94-6239-682-1_7

seismic performance. However, steel substations have increasingly exhibited certain drawbacks in practice, such as poor durability and susceptibility to corrosion[2]. Moreover, because steel components often consist of multiple layers without the protective encasement of concrete, their high thermal conductivity and specific heat capacity tend to cause cracking and water seepage [3].

Replacing steel substations with concrete structures is therefore an effective solution. Concrete offers superior resistance to corrosion, stability, and waterproofing compared with steel, and has been widely applied worldwide [4]. With rising energy demand and the rapid increase in the number of substations, their building energy consumption has become an important issue. Existing research on building energy consumption and efficiency has focused primarily on equipment optimization. For example, Bajsić et al. [5] proposed a mathematical model for hot-water supply operation without auxiliary energy, which optimized HVAC systems and reduced energy consumption. Kansara et al. [6] studied energy-saving alternatives for a 400 kV substation near a superthermal power plant in Rajasthan, India, evaluating high-efficiency lighting and solar-assisted systems from energy, environmental, and economic perspectives.

Some scholars have explored natural ventilation in substation buildings. Juan C. R. et al. [7]performed numerical simulations of underground substations, analyzing airflow patterns and transformer temperature gradients, and quantified the relationship between airflow rate and transformer heat dissipation. Chris Bibby et al. [8] studied natural ventilation in rooms with high-intensity heat sources, finding that surface heat flux, inlet and outlet sizes and positions, and resistance characteristics strongly affected ventilation performance. Maximiliano Beiza et al. [9] conducted heating experiments on underground substations, validated numerical models, and investigated the effects of flow areas, horizontal and vertical ventilation openings on airflow.

Other studies addressed overall energy consumption and optimization strategies. Hu Hao et al. [10] investigated energy use in a 110 kV substation in cold regions, analyzing electrical consumption of equipment and total loads for offices and living spaces. Ding Bin et al. [11] surveyed indoor substations and simulated energy use with DeST software, comparing measured and simulated results. Chen Wei et al. [12]optimized ventilation in transformer rooms. Zhang Zhen et al. [13] analyzed the influence of window-to-wall ratio, thermal transmittance, air exchange, and internal heat sources on heating energy in cold climates. Internationally, Guilherme Carrilho da Graça et al. [14] studied natural and mechanical ventilation in a Lisbon shopping mall using CFD and EnergyPlus. Duerr Shaun et al. [15] validated EnergyPlus for multiple building scenarios and energy storage simulations. Yun et al. [16] investigated louver shading in office buildings, showing its dual impact on visual comfort and lighting energy.

However, these studies have largely overlooked the energy consumption mechanisms of concrete substations. Existing work is often fragmented and limited in model precision, and has not provided effective design strategies for energy savings. Furthermore, comparative studies between concrete and steel substations remain scarce.

Ladybug Tools, an open-source environmental analysis plugin, can import standard EPW weather files to simulate regional climate parameters. Its energy modeling core, EnergyPlus, is widely validated and accepted. The Grasshopper parametric platform integrates algorithms, simulations, and building models, and can link with Radiance

and CFD for comprehensive energy analysis under solar radiation, thermal, humidity, and wind conditions, yielding realistic results.

Based on this, the present study uses Grasshopper and Ladybug Tools to analyze substation energy consumption with three objectives: (1) comparing thermal bridging between steel and prefabricated concrete substations; (2) analyzing baseline energy consumption of standardized 110 kV substations in representative Chinese climate zones and identifying optimization factors; and (3) quantifying the effects of optimization factors across climate zones, and developing multi-factor, multi-objective energy-saving strategies for concrete substations validated by both the Hype and NSGA-II algorithms.

2 Establishment of the Energy-Saving Model

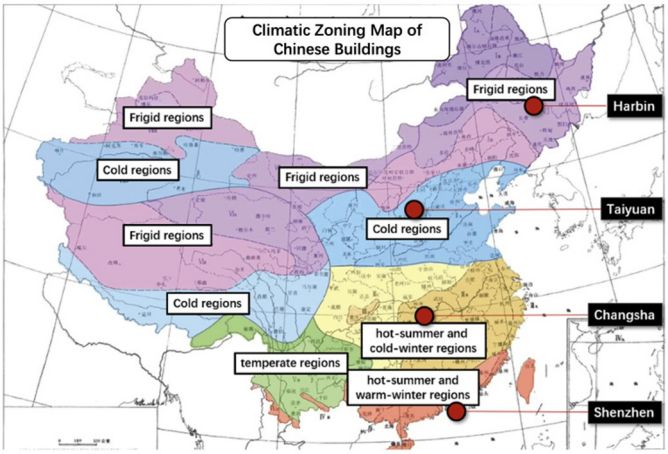

Fig. 1. Test cities and their corresponding climate zones

To investigate the mechanisms of heating and cooling load energy consumption in substations, representative climate zones were first selected for site modeling. The pilot project is a standardized prefabricated 110 kV concrete substation designed by the State Grid Corporation of China. Four representative cities were chosen—Harbin, Taiyuan, Changsha, and Shenzhen—corresponding to severe cold, cold, hot summer and cold winter, and hot summer and warm winter climate zones, respectively (Figure 1). Meteorological data for these cities were obtained from EPW weather files, including the monthly average dry-bulb temperatures and relative humidity levels for the hottest and coldest months. Due to significant climatic differences, the design parameters for energy efficiency vary greatly among these cities. For instance, substations in hot-summer–cold-winter regions such as Changsha must balance both insulation against heat and protection against cold, whereas those in severe cold regions like Harbin require greater emphasis on thermal insulation. In addition, the unique internal heat sources from electrical equipment in substations introduce further complexities, which are addressed in subsequent analyses.

2.1 Modeling Configuration

The analytical model is a standardized prefabricated 110 kV concrete substation with a floor area of approximately 1,900 m². Its floor plans and design renderings are shown in Figures 2-4. The model is divided into two zones. Zone I includes the main transformer room and GIS transformer room, which are non–air-conditioned spaces; therefore, heating and cooling loads are not considered, and only the effects of shading and equipment heat disturbance are modeled. Zone II consists of air-conditioned spaces, including the 10 kV distribution room, capacitor room, battery room, and secondary equipment room. For this zone, the power consumption parameters of equipment were collected to analyze HVAC energy demand and explore energy-saving strategies.

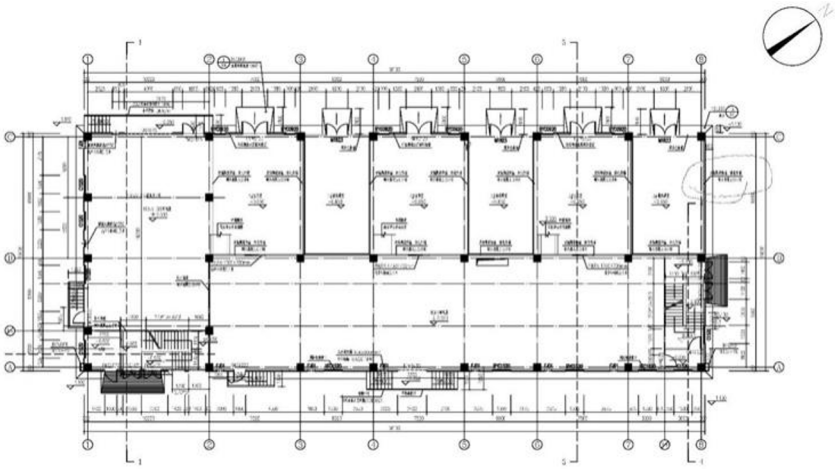

Fig. 2. First Floor Plan of Substation

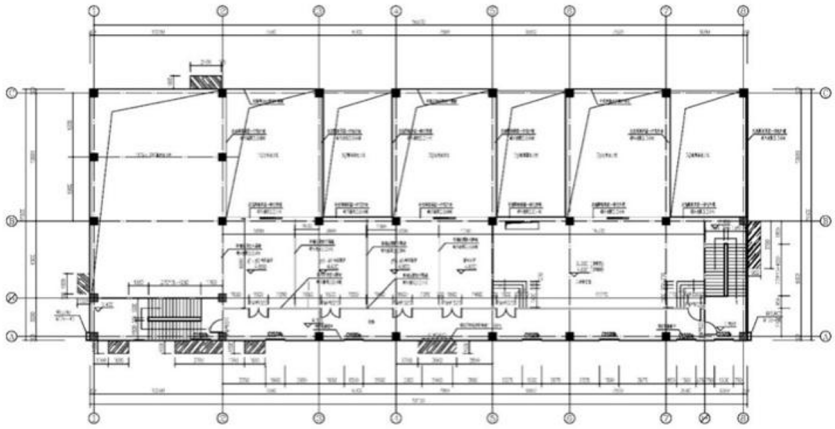

Fig. 3. Second Floor Plan of Substation

Fig. 4. design renderings

For the roof, the assembly from outside to inside consists of: 40 mm fine aggregate concrete + 50 mm extruded polystyrene (XPS) insulation board (thickness adjustable) + 20 mm cement mortar + 120 mm precast concrete slab + 20 mm lime mortar.

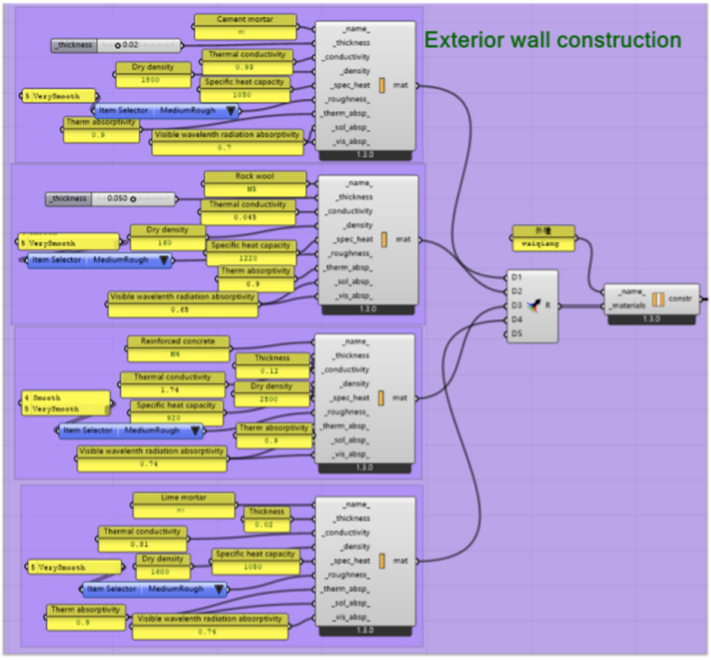

Fig. 5. Exterior wall construction setup

For the exterior windows, single-frame ordinary double-glazing (with thermal-break aluminum alloy frames) was used, with a thickness of (6+12+6) mm. For the floor construction, the layers from top to bottom consist of: 20 mm cement mortar + 80 mm concrete leveling layer + backfill soil. For the interior partition walls, the assembly consists of two 16 mm calcium silicate boards with a 75 mm rock wool core, meeting a two-hour fire-resistance requirement.

This study first compared the thermal performance of envelope structures in substations with steel versus prefabricated concrete systems. In the case of steel construction, the exterior wall was represented by double calcium silicate boards on both sides, with 100 mm vertical and horizontal steel studs in between, and the stud cavities filled with 100 mm of rock wool insulation.

The total thermal resistance of the building envelope is calculated using:

$$R = Re + \sum\left(\frac{\delta 1}{\lambda 1} + \frac{\delta 2}{\lambda 2} + \cdots + \frac{\delta n}{\lambda n}\right) + Ri \quad (1)$$

where R is the overall thermal resistance of the envelope (m²·K/W), Re is the external surface heat transfer resistance (commonly 0.04 m²·K/W), Ri is the internal surface resistance (commonly 0.11 m²·K/W), δn is the thickness of each material layer (m), and λn is the thermal conductivity of each material (W/(m·K)).

For concrete structures, the above formula is applicable since external insulation can effectively neglect thermal bridges. However, in steel structures, due to the high thermal conductivity of the steel studs penetrating the insulation layer, significant thermal bridging occurs, reducing the overall thermal resistance. The horizontal and vertical stud spacing was set at 0.5 m. Therefore, Therm software was employed to simulate the actual thermal transmittance (K-value) of the steel wall (Figure 5).

With an indoor setpoint of 18 °C and outdoor design temperature of 0.9 °C (based on the Design Code for Thermal Insulation of Civil Buildings), the thermal flux distribution and K-value were obtained. The calculated K-values for the steel wall, with and without thermal bridging, were 0.82 and 0.40 W/m²·K, respectively. Thus, the effective K-value was taken as 0.82 W/m²·K, yielding an overall thermal resistance of 1.22 m²·K/W , which is equivalent to that of the concrete wall system with external insulation.

The cooling load of the exterior wall was calculated using:

$$Q\tau = K \cdot A \cdot (tc - tr) \quad (2)$$

where Qτ is the hourly cooling load of the wall (W), K is the overall heat transfer coefficient (W/m²·K), A is the wall area (m²), tc is the outdoor calculation temperature (°C), and tr is the indoor calculation temperature (°C).

This comparison indicates that, in terms of thermal performance, concrete walls require only 50 mm of rock wool insulation to achieve nearly the same performance as steel walls with 100 mm of insulation, highlighting the economic advantage of prefabricated concrete substations.

3 Simulation Results and Analysis

Based on the indoor temperature requirements listed in Table 1, the heating and cooling loads were calculated. In engineering practice, the design of insulation layers typically exceeds the minimum requirements of building codes. Since the thermal transmittance requirements of the building envelope vary across climate zones, the insulation thickness of exterior walls and roofs for each representative city was determined according

to the *General Code for Energy Conservation and Renewable Energy Utilization in Buildings* (see Table 1). Energy consumption simulations were then performed using OpenStudio with the EnergyPlus engine, and the resulting heating and cooling loads for substations in each city are summarized in Table 2.

Table 1. Thickness values of thermal insulation layers in various typical cities

City	Exterior Wall U-value Limit [W/(m·K)]	Wall Insulation Thickness (mm)	Roof U-value Limit [W/(m·K)]	Roof Insulation Thickness (mm)
Harbin	≤ 0.40	110	≤ 0.35	90
Taiyuan	≤ 0.65	60	≤ 0.55	60
Changsha	≤ 1.10	30	≤ 0.70	40
Shenzhen	≤ 1.50	20	≤ 0.90	30

Table 2. Annual Combined Cooling and Heating Loads for Substations Across Cities

Substation city	Annual Cooling Load (kWh)	Annual Heating Load(kWh)	Total Load (kWh)
Harbin	69626.88	0	69626.88
Taiyuan	76,584.49	0	76,584.49
Changsha	83,066.64	0	83,066.64
Shenzhen	99,428.02	0	99,428.02

The results indicate that, due to substantial internal heat gains from equipment in all rooms, substations across all climate zones exhibit virtually no heating load. By contrast, cooling loads dominate in summer, with energy use concentrated in the three capacitor rooms and the secondary equipment room. Moreover, hotter climates incur higher HVAC energy consumption. Therefore, reducing annual cooling demand should prioritize enhancing heat removal from spaces housing high-intensity heat sources.

4 Energy-Saving Optimization Strategies

For this 110 kV substation, the overall form is constrained by prefabricated standardized components, construction processes, fire evacuation codes, and site boundary conditions, leaving little room for further geometric optimization. In addition, the selection of major heat-generating equipment and HVAC systems has already been determined and cannot be altered. Therefore, the proposed energy-saving strategies focus on five key aspects: (1) insulation thickness of the building envelope, (2) window-to-wall ratio, (3) overall building orientation, (4) angle of external shading panels, and (5) air exhaust velocity for mechanical ventilation. The optimization approach is based on the established energy consumption model, with simulations carried out across appropriate parameter ranges to evaluate the effect of each factor on energy-saving rates. This analysis provides insight into how different factors influence substation energy efficiency in various climate zones and enables the prioritization of influencing factors according to their relative impact.

The single-factor energy-saving rate is calculated as:

$$Qesr=(qiec-qoec)/\ qiec*100\% \tag{3}$$

where Q_{esr} denotes the energy-saving rate, q_{iec} the initial energy consumption, and q_{oec} is the optimized energy consumption.

4.1 Insulation Thickness

Insulation thickness has a significant impact on energy performance. In this study, the thickness of the insulation layer was first determined according to the prescribed thermal transmittance (K-value) of the building envelope, which was used as the baseline. The energy-saving rate was then calculated based on simulation results under varying insulation thicknesses, with increments set at 10 mm, a common engineering practice.

Simulation results revealed that the optimal insulation thickness for the standardized substation in Harbin, Taiyuan, and Changsha did not align with the normative values, and in fact, was considerably lower in some cases. Using the standard values as a baseline, the maximum energy-saving rate reached 21.9% in Harbin, 26.8% in Taiyuan, and 7.7% in Changsha, as shown in Figures 6-9.

These findings suggest that in northern China's severe cold and cold regions, internal equipment heat generation strongly influences building thermal performance. Therefore, the K-value standards for building envelopes in substations differ substantially from those of conventional industrial buildings, and the optimal values should be determined through rigorous simulation analysis rather than by directly adopting existing industrial codes.

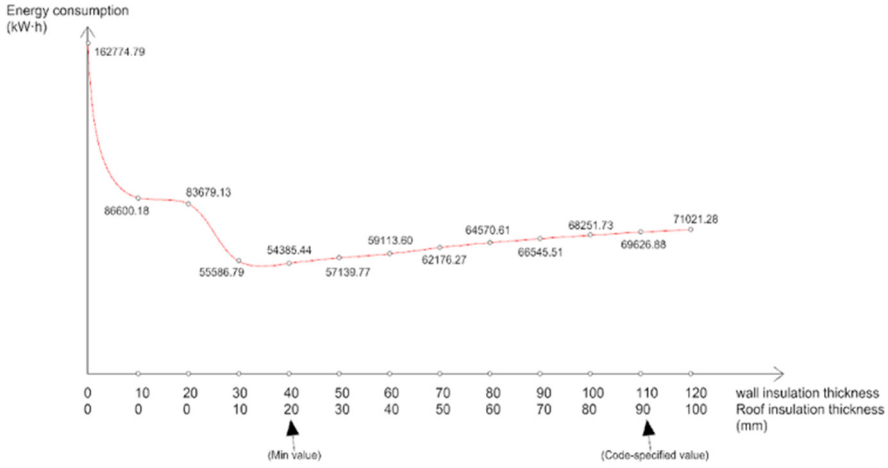

Fig. 6. Insulation Thickness vs. Energy Efficiency in Harbin Substations

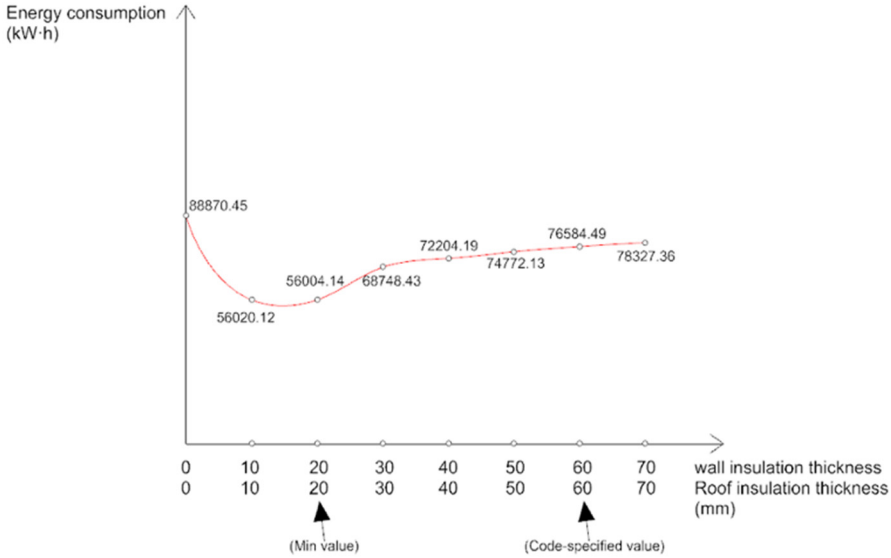

Fig. 7. Insulation Thickness vs. Energy Efficiency in Taiyuan Substations

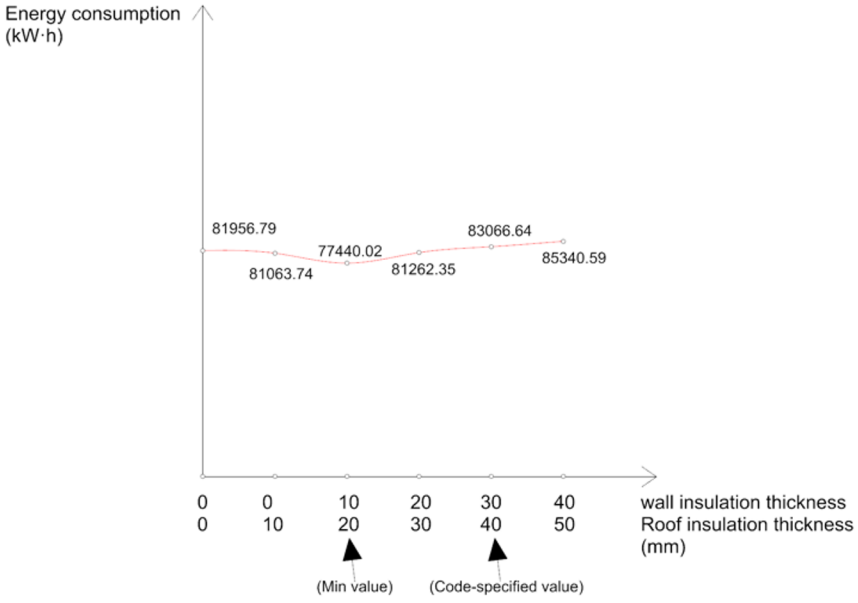

Fig. 8. Insulation Thickness vs. Energy Efficiency in Changsha Substations

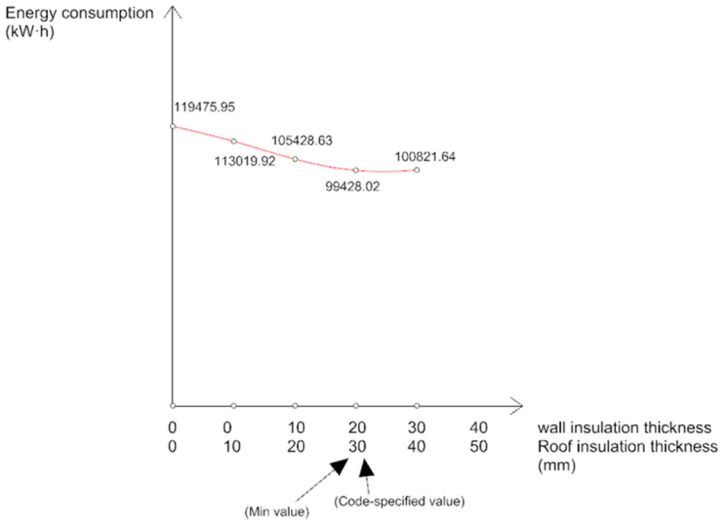

Fig. 9. Insulation Thickness vs. Energy Efficiency in Shenzhen Substations

4.2 Other Parameters (Window-to-Wall Ratio, Building Orientation, Fenestration Shading, Mechanical Ventilation)

Regarding the window-to-wall ratio (WWR), smaller windows in traditional buildings typically improve energy efficiency but sacrifice daylighting. Taking Shenzhen, a city with optimal sunlight conditions, as an example, this study found that in a substation building, only the second-floor corridor achieved 100% effective daylight illuminance (UDI) duration (over 100 lux), while all other areas maintained above 80%. Therefore, sacrificing daylighting to reduce energy consumption is not recommended, and existing window sizes should remain unchanged.

This study employed a single-objective genetic algorithm optimization method to explore the impact of building orientation, fenestration shading, and mechanical ventilation on energy efficiency.

For building orientation, the baseline model was set to a true north-south orientation (a typical orientation commonly found in Chinese architectural design). Energy-saving optimization was performed within a range of −10° to 10°, with 1° intervals.

For the fenestration shading design, the shading device length was aligned with the standard door and window width to balance shading performance with facade aesthetics. All horizontal projections were set to 0.8 m (see Figure 11). The sunshades on the south, east, and west facades are independently adjustable from 0° to 45° (0° being horizontal), ensuring optimal shading in all directions.

For mechanical ventilation, the airflow rate tested ranged from 0 to 1 m^3/s, increasing in 0.1 m^3/s increments. The system automatically activates when the indoor temperature reaches 25–28°C.Table 3 summarizes the maximum single-factor energy savings for substations in different cities.

Table 3. Maximum single-factor energy-saving rates of substations in different cities

Substation Location City	Thermal Insulation Layer Thickness	Orientation of the building	Window Shading	Mechanical Ventilation
Harbin	21.89%	0.0041%	0.010%	80.73%
Taiyuan	26.87%	0.0041%	0.14%	80.30%
Changsha	6.77%	0.0001%	0.19%	24.55%
Shenzhen	0	0.0005%	0.33%	-8.61%

4.3 Analyzing the Impact of Multi-Factor Coupling Effects on Energy Efficiency

We plan to cross-validate the results using two multi-objective optimization algorithms.—The Hype algorithm and the NSGA-II algorithm were used to analyze the energy efficiency performance of a 110 kV precast concrete substation in Changsha under multi-factor coupling conditions.

The two algorithms used the same population size, number of iterations, crossover probability, and mutation probability. The specific parameters are shown in Table 4..

Table 4. Parameters used in the genetic algorithm

Population size (individuals)	Generation Count	Crossover Probability	Mutation Probability
40	50	90%	10%

This optimization framework establishes three core objectives: first, minimizing total energy consumption (as the primary optimization objective); second, maximizing the photovoltaic power generation potential of the sunshade (in line with China's current policy direction of promoting the integration of renewable energy into substations); and third, minimizing construction costs (based on practical engineering economic requirements).

The optimization results are categorized into four types: G1 is the optimal energy solution (lowest energy consumption); G2 is the optimal cost solution (lowest combined expenditure on insulation and photovoltaic materials); G3 is the solution with the highest photovoltaic potential; and G4 is the overall optimal solution. The calculation formula is: $G4 = (E_0 - E_{min})d \cdot n + n \cdot P_t - M_p$. Here, E_0 represents the annual baseline energy consumption (kWh), E_{min} represents the annual optimal energy consumption, d is the unit electricity price (calculated based on Changsha's industrial electricity price of 0.88 yuan/kWh), n is the five-year payback period, and P_t is the photovoltaic potential. In the Pareto front solution set, the system will select the solution with the largest G4 value as the comprehensive optimal solution, and the optimal result of G1–G3 can be obtained directly from the optimization output.

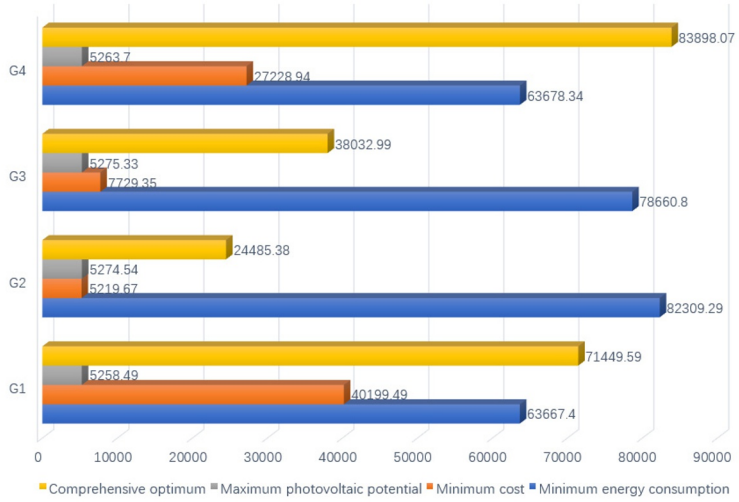

Fig. 10. Four-dimensional optimization results obtained using the Hype algorithm

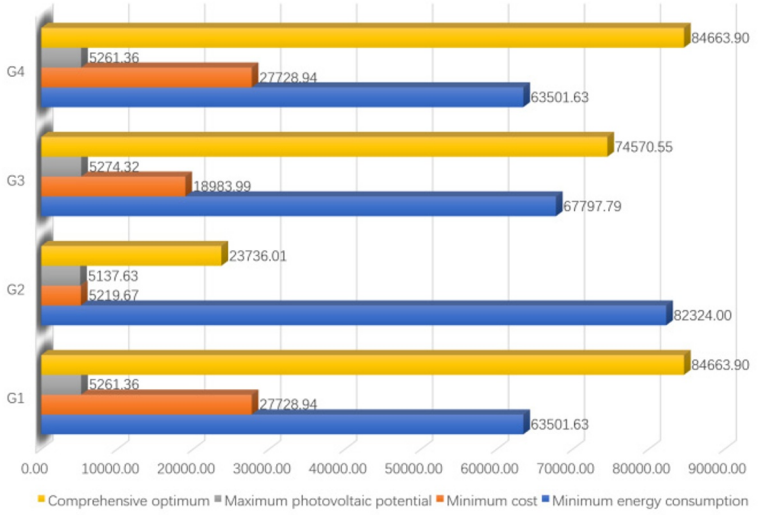

Fig. 11. Optimal results in four dimensions extracted via the NSGA-II algorithm

The iterative results shown in Figures 10 and 11 show that the differences between the two algorithms are minimal: for minimum energy consumption (G1), the difference is only 0.26%; for minimum cost (G2), the results are completely consistent; for maximum photovoltaic potential (G3), the difference is 0.02%; and for maximum five-year return (G4), the difference is 0.91%. These results provide preliminary validation of the accuracy of the method used in this study.

Furthermore, extensive test results demonstrate that the NSGA-II algorithm consistently outperforms the Hype algorithm on two key objectives: minimizing energy consumption (G1) and maximizing five-year comprehensive returns (G4). This performance advantage is primarily attributed to NSGA-II's non-dominated sorting mechanism and crowding distance calculation method, which more effectively retain high-quality solutions. In contrast, the Hype algorithm relies on hypervolume indicators, which slightly reduce the search efficiency of its subsampling process in high-dimensional multi-objective spaces (particularly evident in the three-objective optimization framework of G4), thus demonstrating certain limitations.

5 Conclusion

Main conclusions of this study are as follows:

1. Based on China's current energy efficiency standards, substations in all four climate zones—Harbin (severe cold), Taiyuan (cold), Changsha (hot summer and cold winter), and Shenzhen (hot summer and warm winter)—exhibited no heating load throughout the year, only cooling loads. In general, the higher the latitude, the lower the total annual cooling demand.
2. When thermal bridges are fully considered, the K-values of common envelope structures in prefabricated concrete and steel substations can be regarded as equivalent. Steel structures require 100 mm of rock wool insulation, whereas concrete structures achieve the same thermal performance with only 50 mm, thus offering superior cost-effectiveness.
3. In terms of energy-saving potential, northern (colder) regions showed greater optimization space compared with southern (warmer) regions. The influencing factors on energy efficiency ranked as: mechanical ventilation > insulation thickness optimization > shading panel configuration > building orientation adjustment. Considering both daylighting and energy efficiency, window-to-wall ratio should remain unchanged under standardized design.
4. Using Changsha as a case study, multi-objective optimization with both Hype and NSGA-II algorithms demonstrated that with mechanical ventilation at 0.3 m^3/s, external wall insulation thickness of 40 mm, roof insulation thickness of 20 mm, photovoltaic shading panels angled at 39° (east), 37° (west), and 31° (south), and building orientation at –1°, the maximum energy-saving rate reached 23.55%. Considering economic returns, the same configuration achieved cost payback within five years. The same methodology can be applied to other cities to identify optimal integrated strategies.
5. NSGA-II outperformed the Hype algorithm by maintaining better solution quality through non-dominated sorting and crowding distance. It achieved a stronger balance between convergence and diversity when optimizing energy, cost, and photovoltaic objectives. In contrast, the Hype algorithm's reliance on hypervolume indicators slightly reduced efficiency in high-dimensional cases, making NSGA-II more suitable for substation energy optimization.

Acknowledgement

Project Type: Science and Technology Project of Hunan Electric Power Co., Ltd., Project No.: 5216A2240007

Project Title: Research and Application of Green Intelligent Construction System and Resource Recycling Technology for Prefabricated Concrete Structure Substations

References

1. Bajsić I, Bobič M: Modelling and experimental validation of a hot water supply substation. Energy and Buildings 2006, 38(4):327-333.
2. Bastos Porsani G, Casquero-Modrego N, Echeverria Trueba JB, Fernández Bandera C: Empirical evaluation of EnergyPlus infiltration model for a case study in a high-rise residential building. Energy and Buildings 2023, 296.
3. Bastos Porsani G, Fernández Bandera C: A Case Study of Empirical Validation of EnergyPlus Infiltration Models Based on Different Wind Data. Buildings 2023, 13(2).
4. Beiza M, Ramos JC, Rivas A, Antón R, Larraona GS, Gastelurrutia J, de Miguel I: Zonal thermal model of the ventilation of underground transformer substations: Development and parametric study. Applied Thermal Engineering 2014, 62(1):215-228.
5. Bibby C, Hodgson M: Prediction study of factors affecting speech privacy between rooms and the effect of ventilation openings. Applied Acoustics 2013, 74(4):585-590.
6. Brockhoff D, Bader J, Thiele L, Zitzler E: Directed Multiobjective Optimization Based on the Weighted Hypervolume Indicator. Journal of Multi-Criteria Decision Analysis 2013, 20(5-6):291-317.
7. Candeias M, Obiala R, Demonceau JF, Dinu F, Marginean I, Weynand K: Robustness evaluation and design of steel and steel-concrete buildings according to current standards and recent research results. ce/papers 2023, 6(3-4):2108-2113.
8. Chen C, Wang M, Shen C, Huang Y, Zhu M, Wang H, He L, Julien DB: Sensitivity Analysis of Factors Influencing Rural Housing Energy Consumption in Different Household Patterns in the Zhejiang Province. Buildings 2023, 13(2).
9. Novoselac A, Burley BJ, Srebric J: Development of new and validation of existing convection correlations for rooms with displacement ventilation systems. Energy and Buildings 2006, 38(3):163-173.
10. Ramos JC, Beiza M, Gastelurrutia J, Rivas A, Antón R, Larraona GS, de Miguel I: Numerical modelling of the natural ventilation of underground transformer substations. Applied Thermal Engineering 2013, 51(1-2):852-863.
11. Reilly A, Kinnane O: The impact of thermal mass on building energy consumption. Applied Energy 2017, 198:108-121.
12. Shen T, Shen X: Analysis of Economic Thickness and the Suitable Insulation Thickness of External Wall Insulation Layer. IOP Conference Series: Earth and Environmental Science 2021, 719(2).
13. Vitorino RM, Jorge HM, Neves LP: Multi-objective optimization using NSGA-II for power distribution system reconfiguration. International Transactions on Electrical Energy Systems 2015, 25(1):38-53.
14. Wang M, Chen C, Fan B, Yin Z, Li W, Wang H, Chi Fa: Multi-Objective Optimization of Envelope Design of Rural Tourism Buildings in Southeastern Coastal Areas of China Based on NSGA-II Algorithm and Entropy-Based TOPSIS Method. Sustainability 2023, 15(9).

15. Yun G, Park DY, Kim KS: Appropriate activation threshold of the external blind for visual comfort and lighting energy saving in different climate conditions. Building and Environment 2017, 113:247-266.
16. Zhang XH, Liu JX, Zhang HZ: Analysis on Hot summer and Cold Winter Areas of the Thermal Bridge Hybrid Structure. Applied Mechanics and Materials 2012, 204-208:986-989.